

# Extraction of Stomach Fold Regions from Abdominal X-Ray CT Images Using 3D Top-Hat Transformation

Shigeto Watanabe,<sup>1</sup> Jun-ichi Hasegawa,<sup>1</sup> Yoshito Mekada,<sup>2</sup> Kensaku Mori,<sup>3</sup> and Shigeru Nawano<sup>4</sup>

<sup>1</sup>Graduate School of Computer and Cognitive Sciences, Chukyo University, Toyota, 470-0393 Japan

<sup>2</sup>Graduate School of Engineering, Nagoya University, Nagoya, 464-8603 Japan

<sup>3</sup>Research Center for Advanced Waste and Emission Management, Nagoya University, Nagoya, 464-8603 Japan

<sup>4</sup>Department of Radiology, National Cancer Center Hospital East, Kashiwa, 277-8677 Japan

## SUMMARY

This paper presents a method for extracting stomach wall fold regions from abdominal X-ray CT images using three-dimensional morphology operations. The phenomenon of stomach wall folds concentrating in the direction of lesions is observed in over 60% of stomach cancer patients. Thus, the running pattern of stomach wall folds is an important clue in diagnosing stomach cancer. The method proposed in this paper is composed of three steps of preliminary processing, fold enhancement, and fold extraction and uses three-dimensional top-hat transformation which is a kind of light-dense morphology operations in the enhancement step. Better results than those obtained in the past have been obtained by applying the proposed procedure to nine cases of actual CT images. In addition, effects of differences in imaging environments on the extraction results have been studied in samples in which the body positions during imaging and the amounts of the foaming medium administered orally had been varied. The results obtained provide important findings on the possibility of diagnosing stomach cancer using three-dimensional CT images. © 2004 Wiley Periodicals, Inc. Electron Comm Jpn Pt 2, 87(2): 37–46, 2004; Published online in Wiley InterScience ([www.interscience.wiley.com](http://www.interscience.wiley.com)). DOI 10.1002/ecjb.10214

**Key words:** three-dimensional morphology; top-hat transformation; computer-aided diagnosis; abdominal X-ray CT images; stomach cancer; stomach wall folds.

## 1. Introduction

Medical imaging technology has shown significant advancements in recent years and high-resolution three-dimensional images have been obtained in less time especially with the advent of multislice CT in X-ray CT images. However, while this has made diagnosing human fine body parts possible, it has increased the load of doctors reading the images [1]. Thus, studies on computer-aided diagnoses of CT images have been conducted vigorously [2–5]. Many of the past studies on computer-aided diagnoses of CT images relate to the thorax, and studies on the abdominal areas, especially the stomach, are few. Reasons for this include the following: (1) there have been no urgent needs for CT diagnoses since diagnostic methods based on the gastric endoscopic and stomach X-ray double contrast images have been in existence for stomach cancer in the past, (2) the resolution (especially in the body axis direction) of the past CT images has not been sufficient for reading stomach wall folds, which is diagnostically important. However, as mentioned above, the resolution of CT images

has been steadily improved. In addition, the past stomach X-ray double contrast images require considerable expertise in imaging and cannot avoid overlapping images of the front and back walls of the stomach. Therefore, three-dimensional diagnoses using CT images can be expected to open new possibilities for stomach cancer diagnosis.

With the above-described background, the authors have worked on developing abdominal diagnosis support systems using abdominal X-ray CT images [6–10]. This paper presents the automatic extraction procedure for the stomach wall fold regions, which is a nuclear procedure of their methods. Since the most important step in the procedure is considered to be enhancement of fold regions, the authors have developed procedures that use a three-dimensional rotatory second-order difference or differential filter [11], three-dimensional local curvature characteristics [12], three-dimensional top-hat transformation [13], etc., and have compared their performances [8]. This paper presents the procedure using three-dimensional top-hat transformation, which has given best results among these. In addition, they investigate the effects of differences in the body positions during imaging and the amounts of the foaming agent administered during imaging on the extraction results.

Although there exist other studies on extracting stomach wall folds from CT images, including a study using binary graph top-hat transformation [14] and a study using three-dimensional local curvatures [15], neither has gone beyond preliminary experimental stages. In addition, although examples of applying three-dimensional top-hat transformation to medical images have been published in Refs. 16 and 17, etc., examples of studies conducted with the purpose of extracting stomach wall fold regions like this study are nonexistent. In the remainder of this paper, the stomach wall folds are discussed in Section 2, the detailed extraction procedure is discussed in Section 3, and the experimental results using real multislice CT images are presented in Section 4.

## 2. Characteristics of Stomach Wall Folds

There are many folds running in the shape of mountain ranges on the wall of the stomach [Fig. 1(a)]. There are many comparatively thicker folds on the major curvature side, while there are many thinner folds on the minor curvature side. A concentration of folds in the direction of a lesion is observed when stomach cancer occurs. More than 90% of the caving-in type of cancer, which occurs in 70% of stomach cancer cases, show a concentration of folds [19]. Thus, the stomach folds give important diagnostic information on stomach cancer. When the abdominal area is CT imaged after the oral intake of an appropriate amount of a foaming medium by a patient, dark images of the folds that are almost orthogonal to the slice plane are observed

as protrusions inside the stomach as shown in Fig. 1(b). The clarity of these areas differs depending on the parts of the stomach, the body positions during imaging, the amounts of air inside the stomach, etc. Stomach X-ray double contrast imaging is usually used in observing the stomach folds patterns. This method takes X-ray images of the state of the contrast agents adhering thinly along the folds. In the past, the authors have developed a system of automatically detecting a lesion by quantifying the state of concentration of folds from such stomach X-ray double contrast images [20]. However, estimating the three-dimensional running state of folds from double contrast images is difficult and this is one of the motives for this study.

## 3. Processing Procedure

### 3.1. Outline

The processing procedure proposed here is composed of three steps: (1) preliminary processing, (2) fold enhancement, and (3) fold extraction. To save processing time, the preliminary processing limits the processing range while eliminating air regions outside the stomach that have negative effects on the subsequent steps. The fold enhancement step enhances the protruding regions using three-dimensional top-hat transformation [13], which is a kind of morphology operation [21]. The final fold extraction step extracts fold candidate regions and eliminates unnecessary components with respect to the enhanced image obtained by the preceding steps. Each step is explained in more detail below.

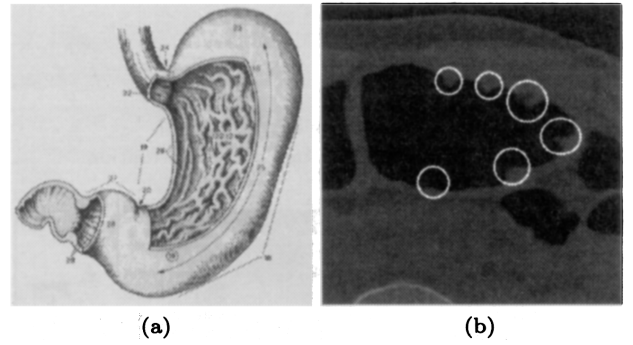


Fig. 1. Stomach fold regions. (a) Sketch of stomach; (b) on the CT image.

### 3.2. Preliminary processing

The preliminary processing is composed of body region extraction, air region extraction, and elimination of air regions outside the stomach.

#### 3.2.1. Body region extraction

Body region extraction is performed as follows.

(a) A binarization procedure is performed for the entire input image such that a shape or form that is greater than an appropriate threshold  $T_1$  ( $= -100$  H.U.) are taken.

(b) The areas having maximum volumes are taken in the three-dimensional binary shapes or forms obtained.

(c) A hole-filling procedure is performed for each slice for the areas obtained as above.

In order to save processing time, all subsequent processing is performed only within the body region area obtained thus.

#### 3.2.2. Air region extraction

Many air regions exist in CT images in areas other than the stomach such as the lungs and the duodenum. In order to extract these, a three-dimensional binary image is obtained by taking the areas that are less than a threshold  $T_2$  ( $= -550$  H.U.) as shapes or forms. The stomach components and components other than these are divided by designating the shape components corresponding to the stomach by manual inputs. The former are referred to as the stomach air regions and the latter as the air regions outside the stomach.

#### 3.2.3. Elimination of air regions outside the stomach

Since there is a possibility that the air regions outside the stomach existing near the stomach wall can adversely influence the results in performing enhancement of the folds by the subsequent step, these regions need to be eliminated beforehand. The eliminating process is as follows:

(a) Perform the form or shape dispersion procedure  $n$  ( $= 4$ ) times on the air regions outside the stomach.

(b) Substitute an average CT value of soft tissues (40 H.U. in the experiments) to each pixel of the CT image corresponding to the regions obtained.

Although the air regions of the stomach cannot be completely eliminated by the above process, the process is considered to be sufficient for the purpose of this study.

### 3.3. Fold enhancement

The overall stomach wall region can be divided into the base part (almost corresponding to the muscular layer) having a comparatively smooth shape and the protruding parts (corresponding to the folds) of a mountain range shape on the base part. As one method of enhancing the fold regions, the method of first obtaining an image representing the above-mentioned base part and subtracting this from the original image is considered. For this, three-dimensional top-hat transformation [13, 20] can be used for the light-dense image.

[Three-dimensional top-hat transformation]

In representing the input dense-light image by a function of three-dimensional coordinates  $\mathbf{x} = (x, y, z)$ , three-dimensional dilation of  $f(\mathbf{x})$  and three-dimensional erosion of  $f(\mathbf{x})$  are defined by Eq. (1) and (2), respectively, with  $g$  as structural elements:

$$[f \oplus g](\mathbf{x}) = \max_{\substack{\mathbf{x}-\mathbf{u} \in F \\ \mathbf{u} \in G}} \{f(\mathbf{x}-\mathbf{u}) + g(\mathbf{u})\} \quad (1)$$

$$[f \ominus g](\mathbf{x}) = \min_{\substack{\mathbf{x}-\mathbf{u} \in F \\ \mathbf{u} \in G}} \{f(\mathbf{x}-\mathbf{u}) - g(\mathbf{u})\} \quad (2)$$

Here,  $F$  and  $G$  are regions defining  $f$  and  $g$ , respectively. Specifically, dilation of a dense-light image dilates the regions with high-density values along the dense-light structure of  $g$  and fills the narrow low-darkness regions. Conversely, erosion dilates the low-density value regions and eliminates the high-density protruding regions or narrow regions. Three-dimensional opening is defined by the following equation using these two operations:

$$f_o(\mathbf{x}) = [(f \ominus g^s) \oplus g](\mathbf{x}) \quad (3)$$

where  $g^s$  is the symmetry function of structural elements  $g$ :

$$g^s(\mathbf{x}) = g(-\mathbf{x}) \quad (4)$$

In other words, since opening performs dilation on the result obtained by performing erosion, while the original image is retrieved overall, high-density narrow regions eliminated by erosion are not retrieved. Thus, protruding regions such as the folds are eliminated among the high-density regions. In addition, structured elements  $g$  are assumed to be a sphere of a uniform darkness of radius  $r_0$ . Thus, three-dimensional opening becomes equivalent to three-dimensional fusion (erosion-dilation type) with the sphere-defining region as the neighborhood.

Finally, three-dimensional top-hat transformation of  $f(\mathbf{x})$  is given by:

$$f_T(\mathbf{x}) = f(\mathbf{x}) - f_o(\mathbf{x}) \quad (5)$$

As a result, only the protruding parts of the high-density regions and the small high-density region part of the input image remain (Fig. 2).

If regions of different densities exist near the air regions of the stomach (such as air regions outside the stomach) in performing top-hat transformation, high-density regions drawn by these regions do not return to the original shapes and as a result, over-picking-up occurs as shown in Fig. 3. The elimination of air regions described in Section 3.2.3 is performed to alleviate this problem.

In addition, the object of processing is only the cube form surrounding the air regions of the stomach obtained in Section 3.2.2.

### 3.4. Fold extraction

An image obtained by the enhancement process of Section 3.3 is binarized by a threshold value determined empirically, which is taken as the fold candidate region. In addition, for this result, components that satisfy at least one of the following two conditions are eliminated as unnecessary components.

- (a) components that are more than a certain distance from the border surface of a stomach air region
- (b) small components whose volumes are less than 10 pixels

The three-dimensional binary form that is obtained is taken as the final fold region. In addition, three-dimensional

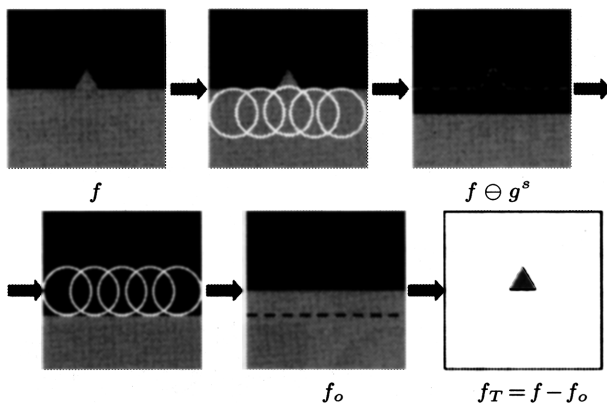


Fig. 2. Illustration of top-hat transformation.

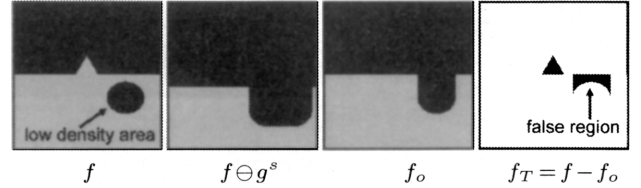


Fig. 3. Illustration of top-hat transformation.

Euclidean distance transformation [22] is used in measuring the distance from the border surface.

## 4. Experimental Results and Discussion

### 4.1. Outline of experiments

Nine abdominal multislice CT images were used in the experiments. The details of the images are shown in Table 1.\*

All images were taken by the same apparatus in the same facility on the same day. Images #1 and #2, #3 and #4, #5 and #6, and #7 and #8 were of the same subjects, respectively. The amounts of the foaming agent administered orally to the subjects for imaging were smaller than the usual dose (8 g). This is due to the fact that in preliminary tests, the usual dose was determined to be inappropriate for observing folds due to the overdistension of the stomach with it.

In the experiments, differences in the extraction results with varying sizes of the structural elements are studied and the optimal size for fold extraction is obtained. Simultaneously, the results with other methods are compared. Next, the effects of differences in the amount of the foaming agent taken orally and differences in the imaged body positions of the subjects are studied.

### 4.2. Study of size of structural elements and comparison with other methods

In order to study the effects of the sizes of the structural elements, which is a major processing parameter of the proposed scheme, on the extraction results, the extraction results of varying the radius  $r_0$  of the element in the range of 2.5 to 12.5 mm (4 to 20 pixels on the slice plane) are compared. An example of the results is shown in Fig. 4.

\* The subject position in the table indicates the body position of the subject during imaging. Supine, prone, decubitus-right, and decubitus-left refer to the body positions of lying down on one's back, lying down with one's face down, lying down with one's left side on the bottom, and lying down with one's right side on the bottom.

Table 1. Specifications of input images used in the experiments

Image No.	Subject Code	Number of slices	Number of pixels	Pixel size (mm)	Slice thickness (mm)	Reconstr. pitch (mm)	Subject position	Foaming medium (g)
1	A	172	512×512	0.625	2	1	supine	4
2	A	183	512×512	0.625	2	1	supine	6
3	B	217	512×512	0.625	2	1	supine	3
4	B	242	512×512	0.625	2	1	supine	5
5	C	152	512×512	0.625	2	1	decubitus-right	4
6	C	208	512×512	0.625	2	1	decubitus-left	4
7	D	183	512×512	0.625	2	1	supine	4
8	D	161	512×512	0.625	2	1	prone	4
9	E	489	512×512	0.625	2	1	supine	4

This image is the result of representing the original image by a volume rendering method incorporating a shading process. Since white color (in the volume rendering method) dark image values are given in advance to the pixels corresponding to the fold regions extracted, the fold regions are seen as white regions in the image. In addition, a shading process is incorporated to make the protruding state of a fold more visible by giving a shade to a fold region. However, since one side of a fold region may be seen dark depending on the positional relationship between the fold region and the virtual light source used in the shading process, the white part and the dark part running adjacent to the white part combined correspond to one fold region. This method is used in all subsequent image representations.

Due to the nature of the scheme, mistakes increase as the size of the structural elements becomes smaller than the width of a fold, whereas losses increase as the size of the structural elements exceeds the width of a fold. This tendency is confirmed also in Fig. 4, and as a result of evaluating the balance between mistakes and losses visually, the appropriate radiiuses for fold extraction have been determined to be 8.75 to 10 mm (14 to 16 pixels on the slice plane).

In addition, it has been found that the angular regions of the stomach are erroneously extracted at a stage in which the structural elements are comparatively small (Fig. 5). This is due to the fact that the three-dimensional density value distribution of the stomach angles is very close to that of the folds. Since the losses cannot be avoided by the

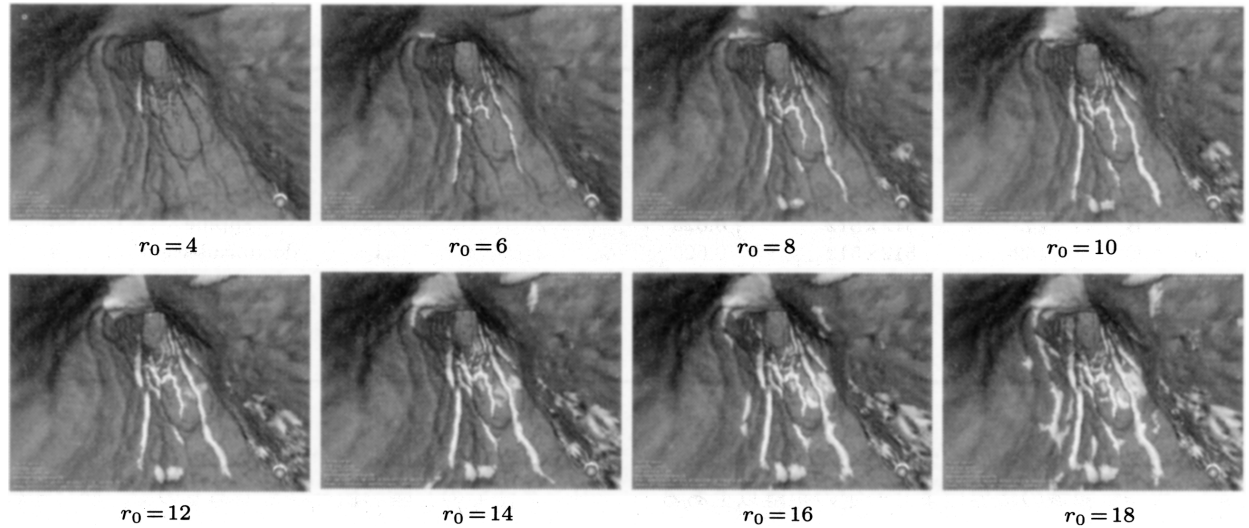


Fig. 4. Results with different values of structural element diameter  $r_0$  (pixels) for Image #4. (Pictures are views of the major curvature area by volume rendering with shading. Fold regions are indicated as white area.)

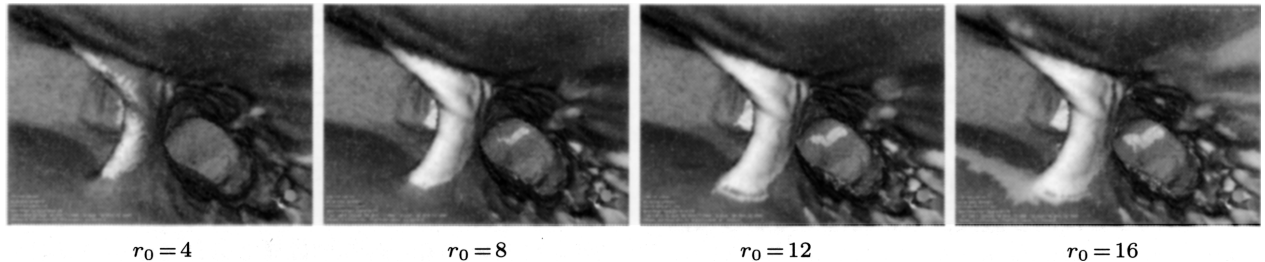


Fig. 5. Results with different values of structural element diameter  $r_0$  (pixels) for Image #4. (Pictures are views of the gastric angle area by volume rendering with shading. Fold regions are indicated as white area.)

proposed scheme, these parts must be extracted by a different method.

For comparison, Fig. 6 shows the results of applying other methods to the same sample. Panels (a) to (c) are the results of using a three-dimensional rotatory second-order difference filter (using the procedure of Ref. 9), the method using a three-dimensional local curvature filter (using the procedure of Ref. 12), and the method using the three-dimensional top-hat transformation of this paper. In the experiments, the radius of the structural elements of top-hat transformation was 10 mm (16 pixels on the slice plane), which has given comparatively good results. In addition, the differential distance of the rotatory second-order differential filter was 5 mm (8 pixels on the slice plane) and the differential distance used in computing the curvature of the local curvature filter was 2.5 mm (4 pixels on the slice plane). First, panel (a) reveals that fold regions are output divided into a number of small regions. This occurs when the widths of the folds are comparatively narrow, and this tendency intensifies further if the differential distance is shortened. This is considered to be an inevitable result, considering that the rotatory second-order difference filter is usually used to enhance mass-shaped regions. The results based on local curvature characteristics of panel (b) show that folds are sufficiently extracted, although many regions connected to this are over-picked-up. This is considered to

be due to the fact that differences in the density values are used in curvature calculations and their errors influence this. Each fold region is well extracted in the results obtained by the proposed scheme of panel (c), and overextraction of the comparatively smooth stomach wall observed in the results obtained by the difference filter and the local curvature filter methods is almost not observed.

The above results confirm the efficacy of the proposed method at least within the scope of the experiments since it is also obtained for other samples used.

#### 4.3. Effects of differences in dose of foaming medium

It has been found from the results of preliminary experiments that very few folds are extracted by the proposed method when the foaming medium is used in the usual dose (8 g). In general, folds are expected to be more visible as the dose of the foaming medium decreases. Thus, extraction experiments have been performed using images #1 to #4 obtained with different doses of the foaming agent under the same conditions. The radius of structural elements  $r_0$  has been fixed at 9.375 mm (15 pixels on the slice plane). Figure 7 shows examples of the experimental results. As a result of evaluating the overall experimental

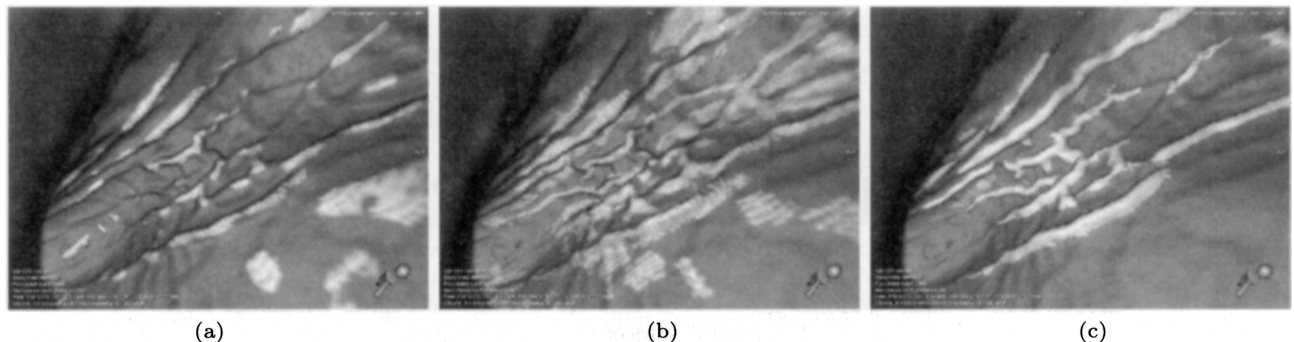


Fig. 6. Comparison of results obtained by three different methods using (a) 3D rotatory second-order difference filter, (b) 3D curvature filter, and (c) 3D top-hat transformation (proposed method).

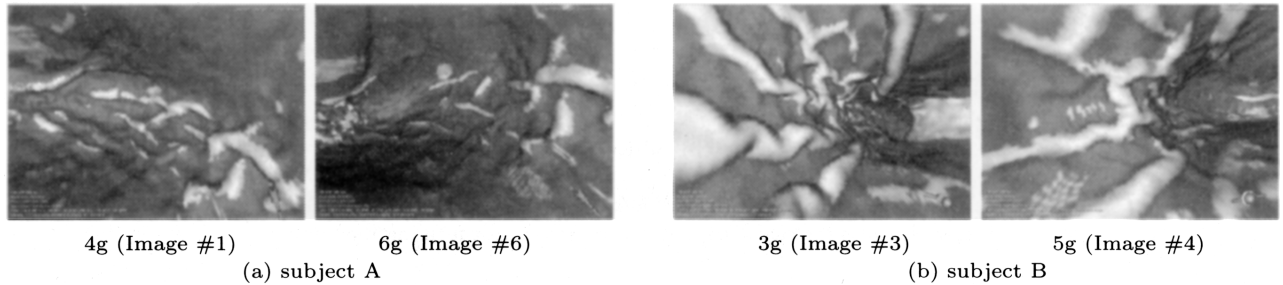


Fig. 7. Results for cases using different amounts of foaming medium.

results visually, the foaming agent in amounts of 4 to 5 g is determined to be appropriate for extracting folds. However, the doses of the contrast medium (barium) and the foaming medium administered to image gastric X-ray double contrast images are currently 200 ml and 1.5 to 2.0 g, and converting 1 g of the foaming medium into 100 ml air yields the overall body volume of 350 to 400 ml. This is interesting, considering that it is nearly the same as the above-mentioned body volume based on the foaming agent and the distension of the stomach is almost the same in the two methods. Since there are individual differences in the size of the stomach and not all of the foaming agent reaches the stomach, controlling stringently the distension of the stomach with the foaming agent is difficult. However, the experimental results on the dose of the foaming agent of this

study may be used as one criterion in abdominal CT diagnoses in the future.

#### 4.4. Effects of differences in body positions during imaging

The extraction results obtained for the images (#5 to #8) taken in varied positions with the amount of the foaming agent fixed at 4 g, with the radius  $r_0$  of the structural elements of 9.375 mm (15 pixels on the slice plane) are compared. Figure 8 shows the experimental results. Comparing panel (a) (1) and (2), it can be seen that the folds are extracted better in the lower parts than in the upper parts for the same position. A similar result is observed in (3) and (4) of panel 8 (a). Next, comparison of (1) and (3) of (a) reveals

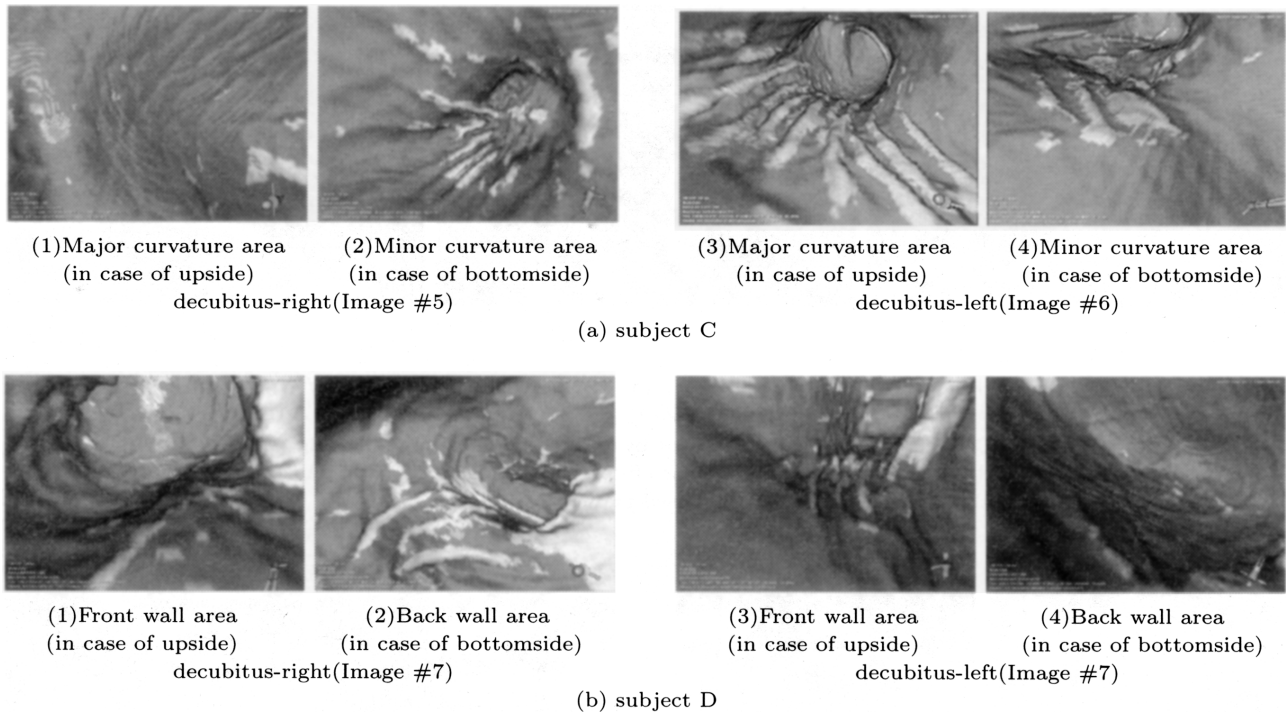


Fig. 8. Results for cases using different amounts of foaming medium.

that shapes differ significantly with different positions even with respect to the same parts of the same subject and more folds are extracted in the lower parts than in the upper parts. Similar results are observed when (2) and (4) are compared. The above tendencies also hold for panel (b). One reason may be that the lower stomach wall does not stretch as easily as the upper wall and folds of the lower wall are more easily extracted. However, gastric juice etc. tends to remain in the lower side and there were a number of parts where extraction could not be obtained due to this effect. Especially in images #5 and #8, gastric juice remains almost spanning the stomach wall (from the vestibular part to the angular part) and folds could not be extracted. Methods for using a multiple number of images of different body positions and methods of imaging that minimize the effects of gastric juice must be developed in the near future.

#### 4.5. Evaluation of extracted results

##### 4.5.1. Evaluation methods

The experimental results are evaluated quantitatively. Since differentiating the fold regions and other regions accurately is in reality difficult even for specialists, a region marked as a fold region manually by one doctor using the method of Ref. 23 on a volume-rendered image is taken as a true fold region in this paper. Folds are classified into three categories (L: large and thick; M: medium; S: small and thin) by their size and thickness. This classification almost corresponds to the clarity of the protrusion of a fold. Next, the extraction results are displayed on the same volume-rendered image, and the degree of extraction of a fold is visually classified into four categories (A: very well extractable; B: extractable; C: not very extractable; D: completely not extractable). Images #4 and #9 were evaluated. These are images taken in the supine position with air amounts of 4 to 5 g, in which many large to small folds are present.

##### 4.5.2. Evaluation results

Table 2 shows the evaluation results. Very good results are obtained for 32 of 35 large folds belonging to category A. There are good results in 77 of 88 larger than

medium folds belonging to categories above B. About 80% of the samples belong to categories lower than C. This is considered to be due to the fact that the sensitivity of the filter could not be raised higher to avoid over-picking-up. An extraction method that suppresses over-picking-up even with increased sensitivities of the filters is needed.

## 5. Conclusions

This paper has presented a procedure for extracting stomach wall fold regions from abdominal X-ray CT images using three-dimensional top-hat transformation, which is a kind of morphology operations. Differences in the extraction results have been compared by applying the procedure to nine cases of abdominal CT images taken in different body positions and with different amounts of the foaming medium. The results show that although there are some individual differences, the optimal amounts of the foaming medium taken orally for imaging are 4 to 5 g. In addition, the extraction results have been found to change significantly with changes in body position. In addition, quantitative evaluations using a part of the samples show that over 90% of folds belonging to medium and higher categories can be extracted. Since these results have been obtained for the first time by this study, it will be an important key to future studies on the abdominal diagnostic possibilities using CT images.

More precise extraction methods, fold region visualization methods, automatic detection of fold-concentrated type cancer lesion candidates using extraction results etc. remain as future study topics.

**Acknowledgments.** The authors extend their sincere thanks to Professor Jun-ichiro Toriwaki of Nagoya University for his daily guidance during this study. They extend the same to various people in Hasegawa's Laboratory at Chukyo University and in Toriwaki's Laboratory at Nagoya University for their enthusiastic participation in discussions regarding this study. This study has been funded partially by the Ministry of Health and Labor Cancer Research Aid Fund, Ministry of Education and Science Private University HRC Aid Fund, and Ministry of Education and Science Scientific Research Promotional Fund.

Table 2. Quantitative evaluation for extraction results

	L	M	S	all
A	32 91.4%	32 65.3%	2 3.7%	66 47.8%
B	2 5.7%	11 22.4%	10 18.5%	23 16.7%
C	1 2.9%	4 8.2%	20 37.0%	25 18.1%
D	0 0.0%	2 4.1%	32 40.7%	24 17.4%
total	35 -	49 -	54 -	138 -

## REFERENCES

1. Katada K. Multislice CT and CAD. Computer Aided Image Diagnostics Society News Letter, No. 29, p 10–19, May 2000.

2. Toriwaki J. Computer aided diagnosis of X-ray images—Study trends and topics. *Trans IEICE* 2000;J83-D-II:3–26.
3. Toriwaki J. A study on the development of a cancer image automatic diagnostic system based on multi-dimensional digital imaging and processing, Ministry of Health Cancer Research Aid Fund Research Result Report. Computer Aided Imaging and Diagnostics Society Papers J (Internet Papers J), Vol. 4, No. 3. <http://www.toriwaki.nuie.nagoya-u.ac.jp/cadm/journal/index.html>
4. Special Issue: Next generational medical imaging technology. *Trans IEICE* 2000;J83-D-II(1).
5. Special Issue: CAD technology. Japanese Radiation Technology Society Magazine 2000;56(3).
6. Wakayoshi N, Hasegawa J, Mekada Y, Nawano S. A preliminary study on correspondence assigning of stomach X-ray TV images and abdominal X-ray CT images. 9th CADM and 8th CAS Conference Joint Papers, p 17–18, 1999.
7. Watanabe S, Hasegawa J, Mekada Y, Mori K, Nawano S. Automatic extraction of stomach inner wall fold regions from abdominal X-ray CT images using a three-dimensional second order differential filter. 9th CADM and 8th CAS Conference Joint Papers, p 19–20, 1999.
8. Watanabe S, Hasegawa J, Mekada Y, Mori K, Nawano S. A comparative study of an automatic method for extracting stomach wall folds from three-dimensional abdominal X-ray CT images. *Tech Rep IEICE* 2000;MI99-50.
9. Watanabe S, Hasegawa J, Mekada Y, Mori K, Nawano S. Additional experiments of stomach wall fold automatic extraction from three-dimensional abdominal X-ray CT images. *Tech Rep IEICE* 2001; MI2000-61.
10. Mekada Y, Mori K, Hasegawa J. Virtual observation of the stomach using two-dimensional and three-dimensional abdominal X-ray CT images. 40th Japanese ME Society Conference Papers, p 202, 2001.
11. Shimizu A, Ukai M, Hasegawa J, Toriwaki J. Performance evaluation of a three-dimensional enhancing filter for lung cancer image detection from three-dimensional chest CT images. *Med Imaging Technol* 1995;13:853–864.
12. Thirion JP, Gourdon A. Computing the differential characteristics of isointensity surfaces. *Computer Vision and Image Understanding* 1995;61:190–202.
13. Meyer F. Automatic screening of cytological specimens. *Computer Vision, Graphics and Image Processing* 1986;35:356–369.
14. Koen K, Mekada Y, Kasuga M. A study on extraction of stomach wall fold regions from abdominal X-ray CT images. 1999 Shingaku General Meeting, D-12-50, p 223.
15. Seki A, Mori K, Suenaga Y, Toriwaki J. Human organ sketch constructing method using three-dimensional curvature information and its application to abdominal CT images. *Med Imaging Technol* 2000;18:595–596.
16. Koryoku T, Kaneko T. Method for extracting abdominal organ regions based on three-dimensional morphology. *Trans IEICE* 1999;J82-D-II:1411–1419.
17. Kubo M, Maki N, Eguchi K, Nakagawa C, Yamaguchi N. A scheme for reducing background bias in chest thin-section CT images. *Trans IEICE* 1999;J82-D-II:2412–2419.
18. Yamada E. (translator). Illustrated dictionary of anatomy, 2nd ed. Igaku Shoin; 1998. p 121.
19. Nawano S, Yamada T, Anami M, Murakami T. Stomach X-ray images and stomach cancer diagnosis. In: Toriwaki J, Tateno Y, Iinuma T (editors). Computer diagnosis of medical X-ray images. Springer; 1994. Section 3.1, p 149–156.
20. Hasegawa J, Tsutsui T, Toriwaki J. Automatic extraction of cancer lesions with concentrated folds in stomach X-ray double contrast images. *Trans IEICE* 1990;J73-D-II:661–669.
21. Obata H. Morphology. Corona Publishers; 1996.
22. Saito T, Toriwaki J. Euclidean distance transformation of three-dimensional digital images. *Trans IEICE* 1993;J76-D-II:445–453.
23. Mori K, Higuchi Y, Suenaga Y, Toriwaki J, Hasegawa J, Katada K. A method of interactive specification of interested regions via a volume rendered image with applications to virtualized endoscope system. *Proc SPIE Conference on Physiology and Function from Multidimensional Images* 2000;3978:134–145.

## AUTHORS (from left to right)



**Shigeto Watanabe** (student member) received his B.S. and M.S. degrees from the Department of Computer Science of Chukyo University in 2000 and 2002 and is currently in the doctoral program. His research interests include three-dimensional medical image processing.

**Jun-ichi Hasegawa** (member) received his B.S. degree from the Department of Electrical and Electronic Engineering of Nagoya University in 1974 and Ph.D. degree in computer science in 1979. After serving as a research associate and lecturer at Nagoya University and an associate professor on the Faculty of Liberal Arts, Chukyo University, he has been a professor on the Faculty of Computer and Cognitive Sciences, Chukyo University, since 1992. His research interests include pattern recognition, image understanding, and their applications to medicine and sports. He is a member of Joho Shori Gakkai, Artificial Intelligence Society, Japanese ME Society, Japanese Medical Imaging Engineering Society, Computer Aided Imaging and Diagnostics Society, and IEEE.

**Yoshito Mekada** (member) received his B.S. and Ph.D. degrees from the Department of Computer Science of Nagoya University in 1991 and 1996 and became a research associate at Utsunomiya University. He has been an associate professor of computer science in the Graduate School of Engineering of Nagoya University since 2001. His research interests include image processing and its medical applications, and signal processing. He is a member of the Japanese Medical Imaging Engineering Society and Computer Aided Imaging and Diagnostics Society.

**Kensaku Mori** (member) received his B.S. and Ph.D. degrees from the Department of Electronic Engineering of Nagoya University in 1992 and 1996. He was a special research member of the Japanese Scientific Research Promotional Society from 1994 to 1997. After serving as a research associate and lecturer in the Graduate School of Engineering, he has been an associate professor in the Research Center for Advanced Waste and Emission Management, Nagoya University, since 2001. He was a visiting associate professor at Stanford University in 2001. His major research interests are applications of computer graphics and three-dimensional image processing to medical images. He received an Encouragement Award, Japanese Medical Imaging Engineering Society; Japanese ME Society Paper Award and Sakamoto Award, Niwa Memorial Award; Information System Society Paper Award from this society; and Japanese Bronchial Society Excellent Topic Award. He is a member of the Japanese ME Society, Japanese Medical Imaging Engineering Society, Computer Aided Imaging and Diagnostics Society, and Japanese Bronchial Society; and affiliate of the IEEE Computer Society and IEEE Engineering in Medicine and Biology Society.

**Shigeru Nawano** received his M.D. degree from the School of Medicine of Chiba University in 1981. He is a member of the Department of Radiology, National Cancer Center Hospital, and head of the Department of Radiology, National Cancer Center Hospital East (radiology specialist, Ph.D.). His research interests include computed radiography, mammography, CAD, MRI, and CT.